Design of Circularly Polarized Microstrip Patch Antenna and 4-Element Array at 8.75 GHz

Santiago Castillo

August 16, 2026

Contents

1 Introduction

This report presents the design, simulation, and analysis of a circularly polarized (CP) microstrip patch antenna operating at a center frequency of 8.75 GHz, along with a 4-element array configuration. The design targets the following specifications:

- Center frequency: 8.75 GHz
- Bandwidth (S_{11} < -10 dB): 8.5 – 9.0 GHz
- Axial ratio < 3 dB at broadside
- RHCP/LHCP realized gain difference $\geq$ 15 dB at broadside

Circular polarization is achieved through a corner-chamfered patch fed by a coaxial probe beneath the ground plane offset from the edge. The single element design is first validated against all specifications before a 4-element array is investigated at element spacings of 0.5λ, 0.75λ, and λ to evaluate mutual coupling and radiation performance. All simulations were performed in Ansys HFSS.

2 Analytical Expressions

2.1 Patch Antenna Design Equations

Before simulation, the theoretical dimensions for the patch antenna were calculated using closed-form design equations. In this design, a Rogers RO3003 substrate was used with a relative permittivity of $\varepsilon_r = 3.0$ and a thickness of $h = 1.52$ mm.

For a conventional rectangular microstrip patch antenna, the width is initially estimated using:

$$W = \frac{c}{2f_r}\sqrt{\frac{2}{\varepsilon_r + 1}} \tag{1}$$

Substituting $f_r = 8.75$ GHz gives $W \approx 12.13$ mm. However, for circular polarization, a square patch geometry is required to support two orthogonal modes (TM_{10} and TM_{01}) with nearly equal resonant frequencies. Therefore, the design enforces $L = W$, and the resonant length expression is used to determine the patch dimensions.

The effective dielectric constant is given by:

$$\varepsilon_{r,\text{eff}} = \frac{\varepsilon_r + 1}{2} + \frac{\varepsilon_r - 1}{2}\left(1 + \frac{12h}{W}\right)^{-1/2} \tag{2}$$

Using an initial estimate for W, the effective dielectric constant is calculated as $\varepsilon_{r,\text{eff}} \approx 2.63$.

The fringing fields at the patch edges extend the effective electrical length beyond its physical length. The length extension is:

$$\Delta L = 0.412h \cdot \frac{(\varepsilon_{r,\text{eff}} + 0.3)\left(\frac{W}{h} + 0.264\right)}{(\varepsilon_{r,\text{eff}} - 0.258)\left(\frac{W}{h} + 0.8\right)} \tag{3}$$

which gives $\Delta L \approx 0.7262$ mm.

The effective resonant length is determined from:

$$L_{\text{eff}} = \frac{c}{2 f_r \sqrt{\varepsilon_{r,\text{eff}}}} \tag{4}$$

yielding $L_{\text{eff}} \approx 10.6$ mm. The physical patch length is then:

$$L = L_{\text{eff}} - 2\Delta L \tag{5}$$

which gives $L \approx 9.11$ mm.

To satisfy the circular polarization requirement, the patch is designed to be square, and thus the final dimensions are chosen as:

$$L = W \approx 9.11 \text{ mm} \tag{6}$$

This ensures that the two orthogonal modes are nearly degenerate, enabling circular polarization when a perturbation (corner chamfer) is introduced. Note: The width expression in (1) is used only as an initial estimate for evaluating $\varepsilon_{r,\text{eff}}$.

2.2 Coaxial Feed Location

In order to match the input impedance to the characteristic impedance of the feed line ($Z_0 = 50\,\Omega$), the coaxial feed is offset from the radiating edge by a distance y_0. The input resistance R_{in} of the patch varies as a function of the inset distance according to the cosine-squared relationship:

$$R_{in}(y_0) = R_{edge} \cos^2\left(\frac{\pi y_0}{L}\right) \tag{7}$$

where R_{edge} is the resonant resistance at the leading edge ($y_0 = 0$) and L is the resonant length of the patch. For the Rogers RO3003 substrate ($\epsilon_r = 3.0$, $h = 1.52$ mm) operating at 8.75 GHz, the edge resistance R_{edge} is calculated to be approximately $160\,\Omega$.

To determine the specific offset required for a $50\,\Omega$ match, the equation is rearranged to solve for y_0:

$$y_0 = \frac{L}{\pi} \cos^{-1}\left(\sqrt{\frac{50}{R_{edge}}}\right) \tag{8}$$

Substituting the design parameters $L = 9.11$ mm and $R_{edge} = 160\,\Omega$, the optimal feed location is found to be:

$$y_0 = \frac{9.11}{\pi} \cos^{-1}\left(\sqrt{\frac{50}{160}}\right) \approx 2.84 \text{ mm} \tag{9}$$

The feed is positioned at this distance from the radiating edge and centered along the patch width ($W/2$) to maintain electrical symmetry and minimize the excitation of unwanted cross-polarized modes.

2.3 Circular Polarization via Corner Chamfer

To achieve circular polarization using a single probe feed, two opposite corners of the square patch are truncated by a length dL. The truncation area Δs is determined by the quality factor Q_0 of the antenna according to the following relationship:

$$\frac{\Delta s}{S} = \frac{1}{2Q_0} \tag{10}$$

where $S = L \times W$ is the total area of the patch. Since $\Delta s = dL^2$ for two symmetric corner cuts, the truncation length is calculated as:

$$dL = L\sqrt{\frac{1}{2Q_0}} \tag{11}$$

For the RO3003 substrate at 8.75 GHz, an estimated quality factor of $Q_0 \approx 40$ yields a truncation length of $dL \approx 1.02$ mm. This perturbation splits the fundamental mode into two orthogonal modes with the required 90° phase shift for circular polarization.

2.4 Summary of Theoretical Dimensions

Table 1 summarizes the theoretical dimensions used to initialize the HFSS model. These dimensions are parameterized as global variables, allowing for automated optimization and parametric analysis. This process ensures the final dimensions are tuned for peak performance before moving to the fabrication stage.

Table 1: Initial Simulation Parameters

Parameter	Variable	Value
Patch width	W	9.11 mm
Patch length	L	9.11 mm
Chamfer cut	dL	1.02 mm from corner
Feed offset	y_0	2.84 mm from edge

3 Single Element Design

In HFSS, the parameters from Table 1 were modified to meet the desired specification of the antennas. The final parameters were obtained through a combination of parametric sweeps and optimization runs.

3.1 Antenna Geometry and Substrate

The final design parameters are summarized in Table 2.

Table 2: Single Element Design Parameters

Parameter	Variable	Value
Substrate material	–	Rogers RO3003
Relative permittivity	ε_r	3.0
Loss tangent	$\tan\delta$	0.0013
Substrate thickness	h	0.508 mm
Substrate size	–	35 × 35 mm
Ground plane size	–	35 × 35 mm
Patch width	W	9.00 mm
Patch length	L	9.25 mm
Chamfer cut	dL	1.8 mm from corner
Feed offset from edge	y_0	2.3 mm
Patch conductor	–	Copper (PEC)

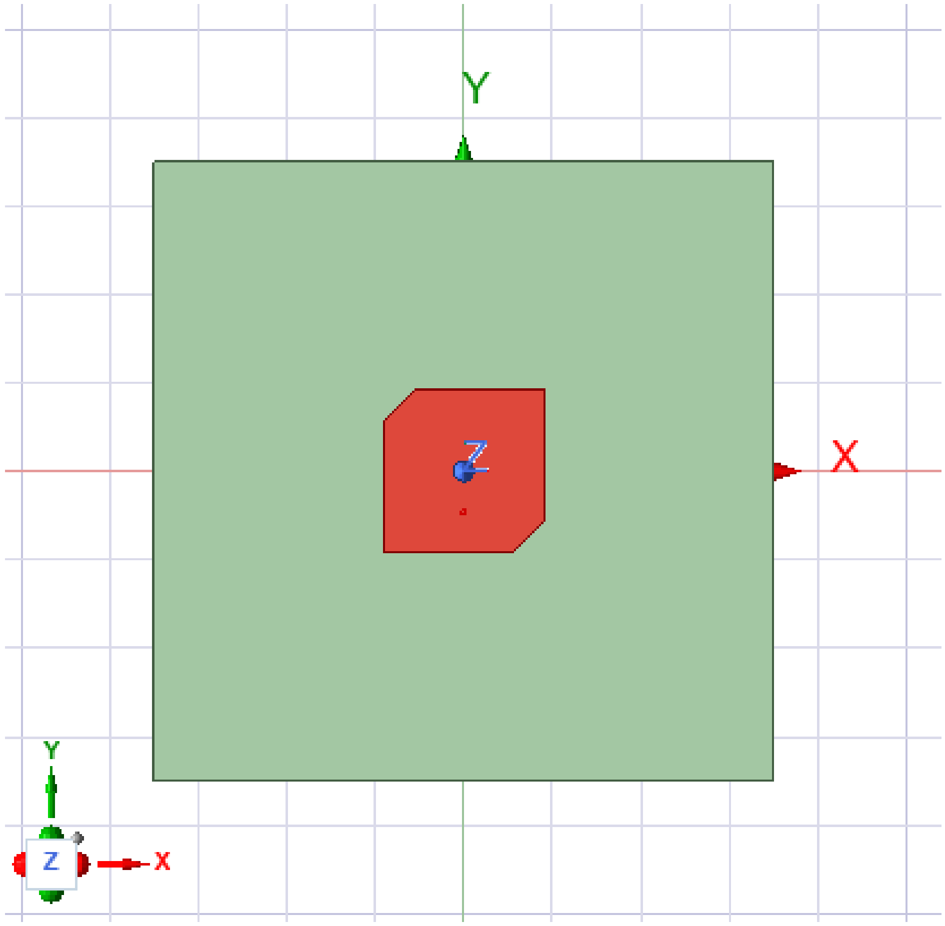

Figure 1: HFSS Design of Single Patch Antenna

Table 3: Single Element HFSS Simulation Settings

Setting	**Value**
Solver	Driven Modal
Solution frequency	8.75 GHz
Frequency sweep type	Discrete
Frequency range	8.0 – 9.5 GHz
Frequency step	5 MHz
Adaptive mesh passes	10
Delta S convergence	0.02
Radiation boundary	$\lambda/4$ clearance all faces
Radiation box size	45 $\times$ 45 mm
Far field resolution	1° in θ and ϕ
Port type	Lumped / Wave port (coaxial)

3.2 S_{11} Parameter

The simulated reflection coefficient of the single element is shown in Figure 2. Two resonant dips are observed at approximately 8.5 GHz and 9.0 GHz, corresponding to the two orthogonal modes introduced by the corner chamfer. Both dips remain below -10 dB, yielding an impedance bandwidth of 8.353 – 9.307 GHz (10.8%), which comfortably exceeds the 8.5 – 9.0 GHz requirement.

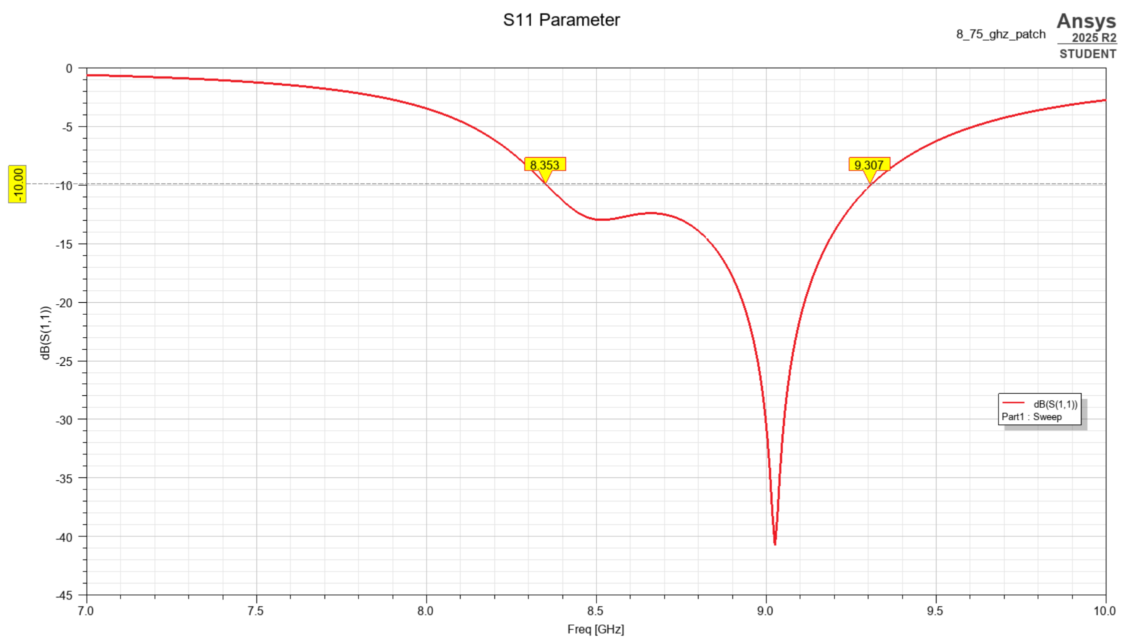

Figure 2: Simulated S_{11} of the single element patch antenna.

3.3 Axial Ratio

The axial ratio was plotted at $\phi = 0°$ and $\phi = 90°$, giving the patterns in the XZ and YZ planes shown in Figure 3. At broadside ($\theta = 0°$), an axial ratio of 2.89 dB was achieved, confirming good circular polarization at the 8.75 GHz design frequency.

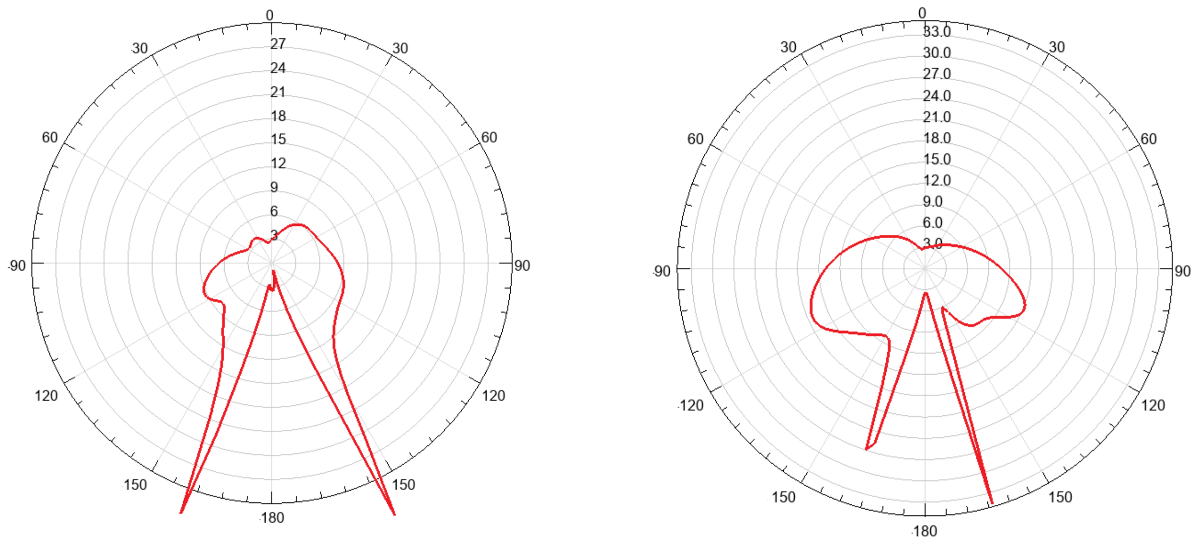

(a) XZ plane ($\phi = 0°$) (b) YZ plane ($\phi = 90°$)

Figure 3: Axial Ratio Values in XZ and YZ Planes

3.4 Circular Polarization Performance

The RHCP and LHCP realized gain patterns in the XZ and YZ planes are shown in Figure 4. At broadside, the RHCP gain exceeds the LHCP gain by 15.68 dB, meeting the polarization difference requirement. The patterns show that the patch is left-hand circularly polarized.

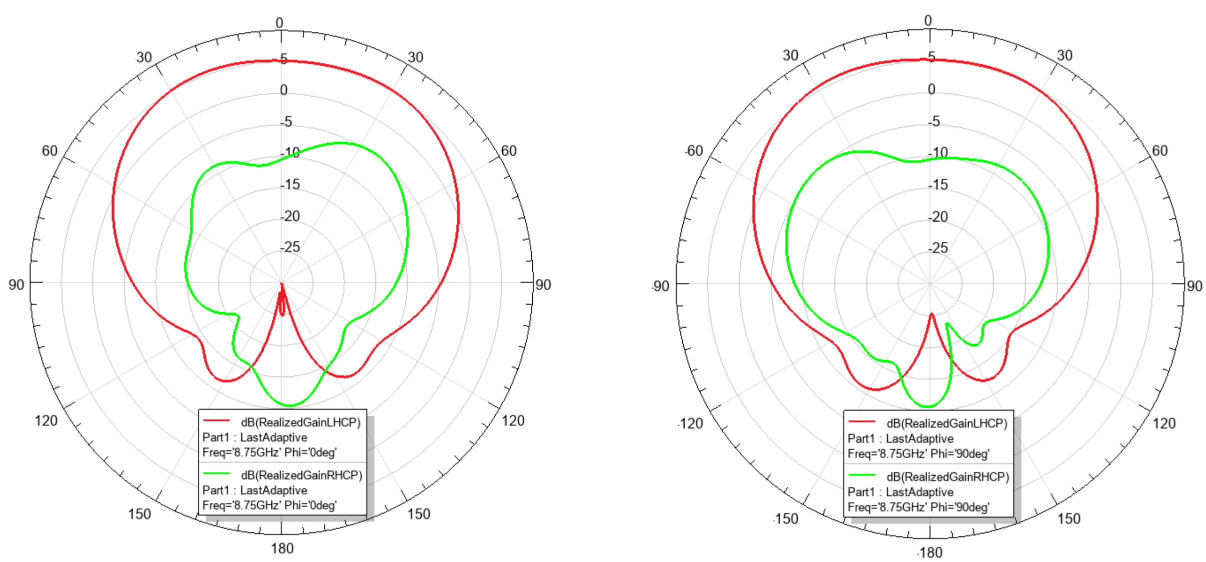

(a) XZ plane ($\phi = 0°$) (b) YZ plane ($\phi = 90°$)

Figure 4: RHCP (green) and LHCP (red) realized gain versus θ

3.5 3D Radiation Patterns

The 3D patterns were plotted for the single element. The maximum realized gain was 6.43 dB at broadside, and the maximum directivity was 6.55 dB at broadside. These plots are shown in Figure 3.

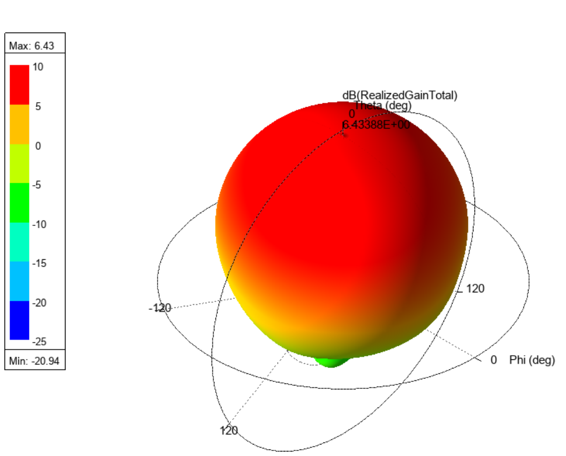

(a) Realized Gain Plot

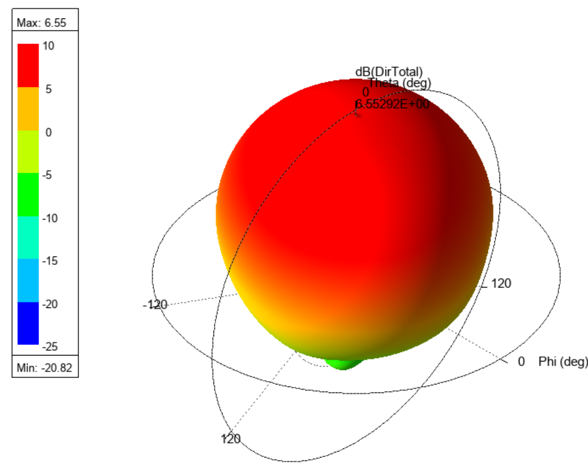

(b) Directivity Plot

Figure 5: 3D Patterns of Single Patch

3.6 Single Element Performance Summary

Table 4: Single Element Simulated Performance vs. Requirement

Parameter	**Requirement**	**Simulated**	**Status**
Center frequency	8.75 GHz	8.83 GHz	✓
Bandwidth	8.5 – 9.0 GHz	8.353 – 9.307 GHz	✓
Axial ratio (broadside)	< 3 dB	2.89 dB	✓
RHCP/LHCP difference	≥ 15 dB	15.68 dB	✓
Realized Gain	–	6.43 dB	–

4 4-Element Array Design

4.1 Array Configuration and Parameters

A 4-element array was then designed using the validated single element as the radiating unit. Each element was fed independently by its own coaxial feed with equal amplitude and phase.

The elements were arranged in a circular configuration and the array radius is evaluated at 0.5λ, 0.75λ, and λ, where:

$$\lambda = \frac{c}{f_0} = \frac{3 \times 10^8}{8.75 \times 10^9} \approx 34.3 \text{ mm} \tag{12}$$

Table 5: Array Geometrical Parameters

Configuration	**Radius (λ)**	**Radius (mm)**
Config. 1	0.5λ	17.15 mm
Config. 2	0.75λ	25.73 mm
Config. 3	λ	34.30 mm

Table 6: Array HFSS Simulation Settings

Setting	**Value**
Solver	Driven Modal
Solution frequency	8.75 GHz
Frequency sweep type	Discrete
Frequency range	8.0 – 9.5 GHz
Frequency step	5 MHz
Adaptive mesh passes	10
Delta S convergence	0.02
Number of ports	4 (one per element)
Excitation	Equal amplitude and phase
Radiation boundary	$\lambda/4$ clearance all faces
Far field resolution	$1°$ in θ and ϕ

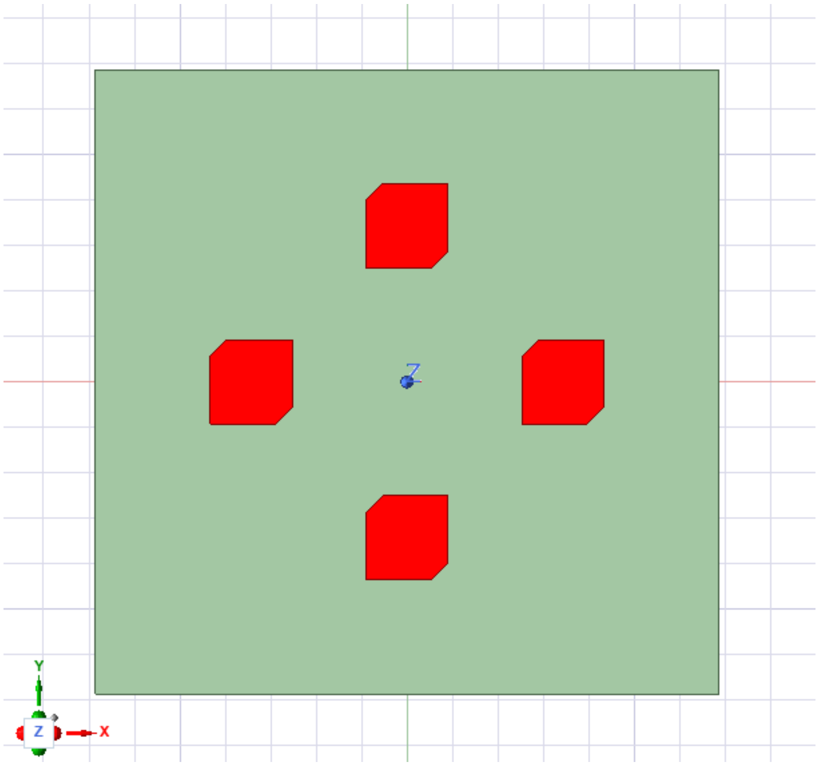

Figure 6: 4-element array geometry in HFSS showing element layout and feed locations.

4.2 Mutual Coupling — S-Parameters

For each array configuration, the S-Parameters were analyzed in the scenarios where only port 1 was excited (Passive) and when all ports were excited (Active). This was done in order to determine the effect of the mutual coupling in the array.

4.2.1 0.5λ Spacing

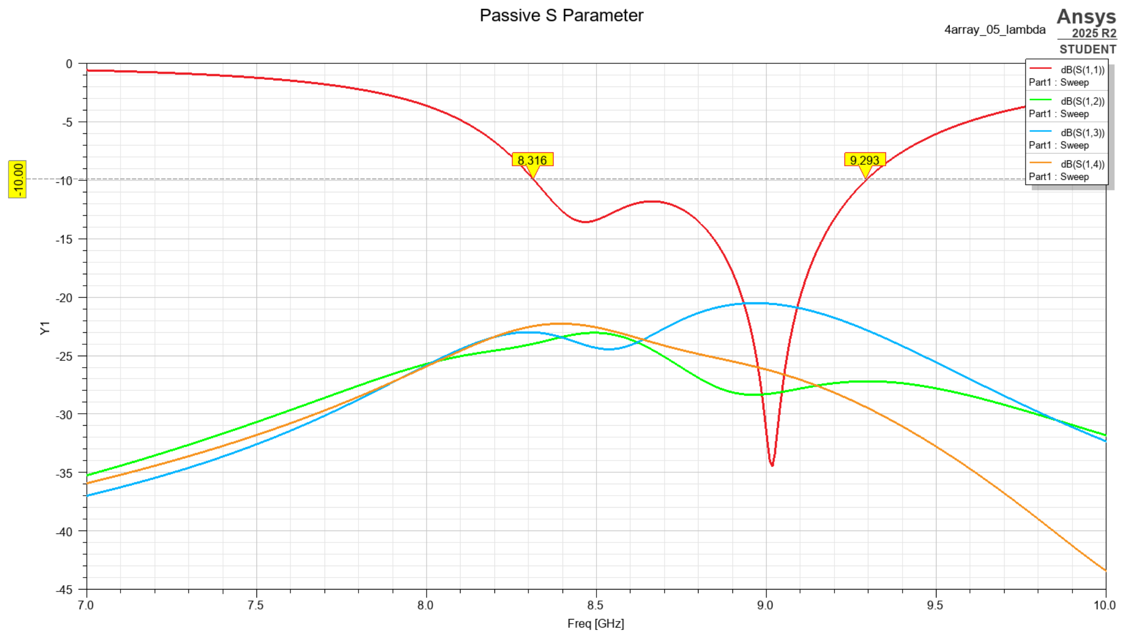

Figure 7: S-Parameter Coupling for Port-1 Excitation at 0.5λ spacing

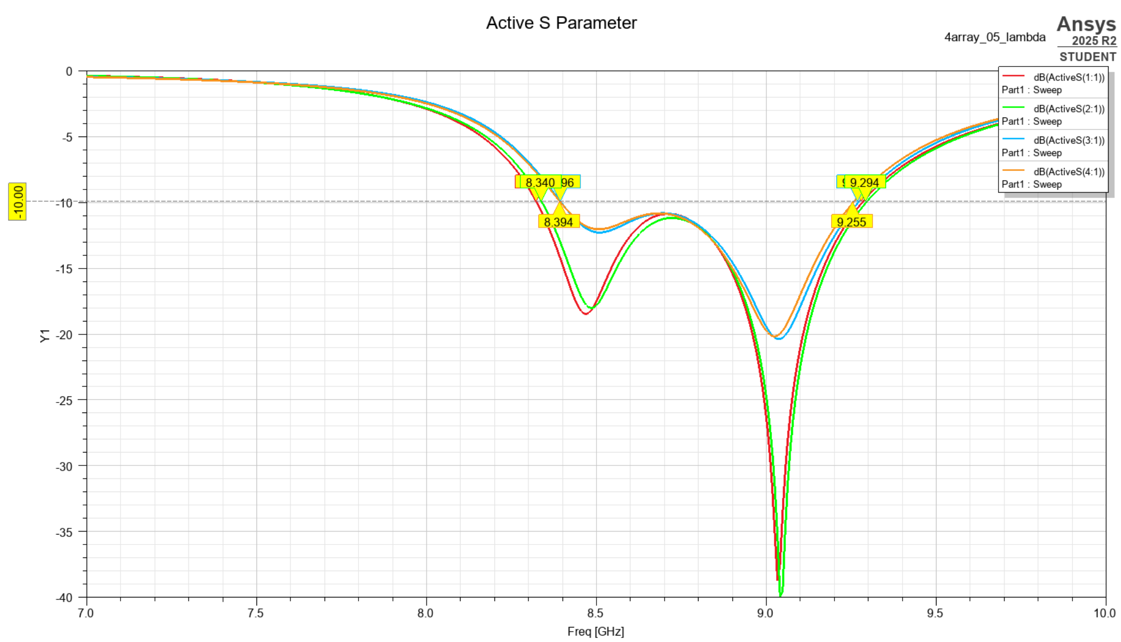

Figure 8: Active S-Parameters at 0.5λ spacing

4.2.2 0.75λ Spacing

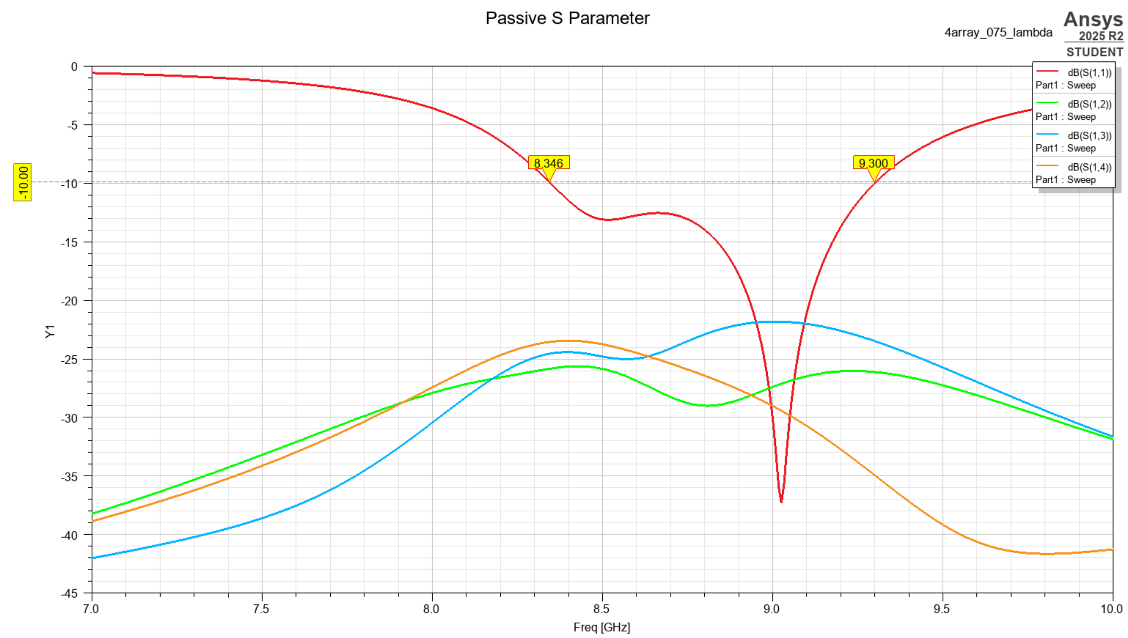

Figure 9: S-Parameter Coupling for Port-1 Excitation at 0.75λ spacing

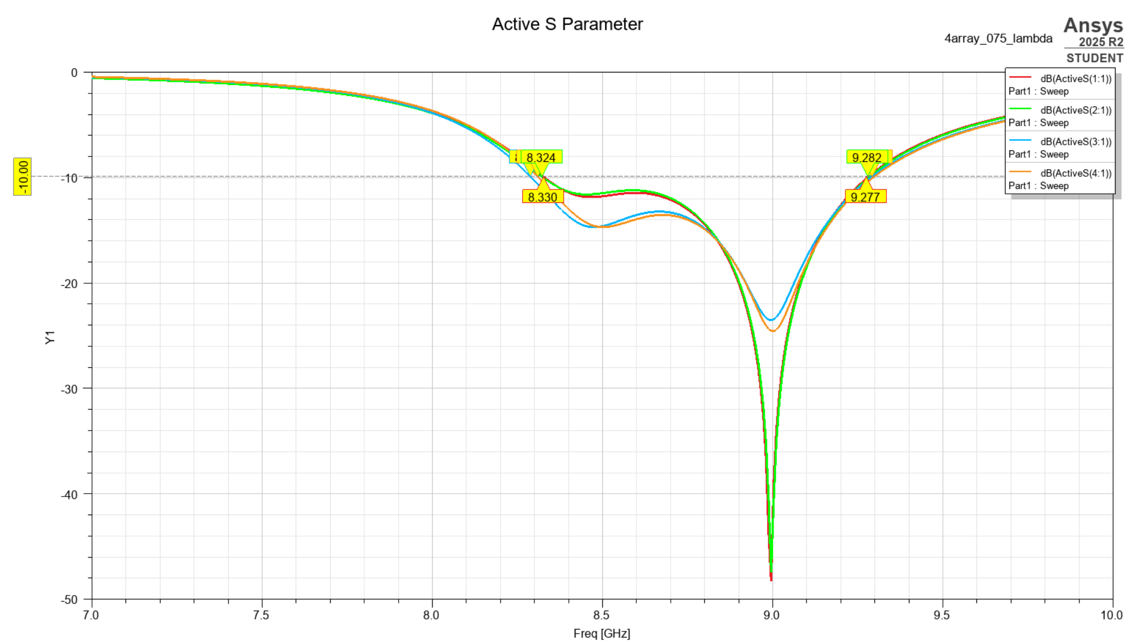

Figure 10: Active S-Parameters at 0.75λ spacing

4.2.3 λ Spacing

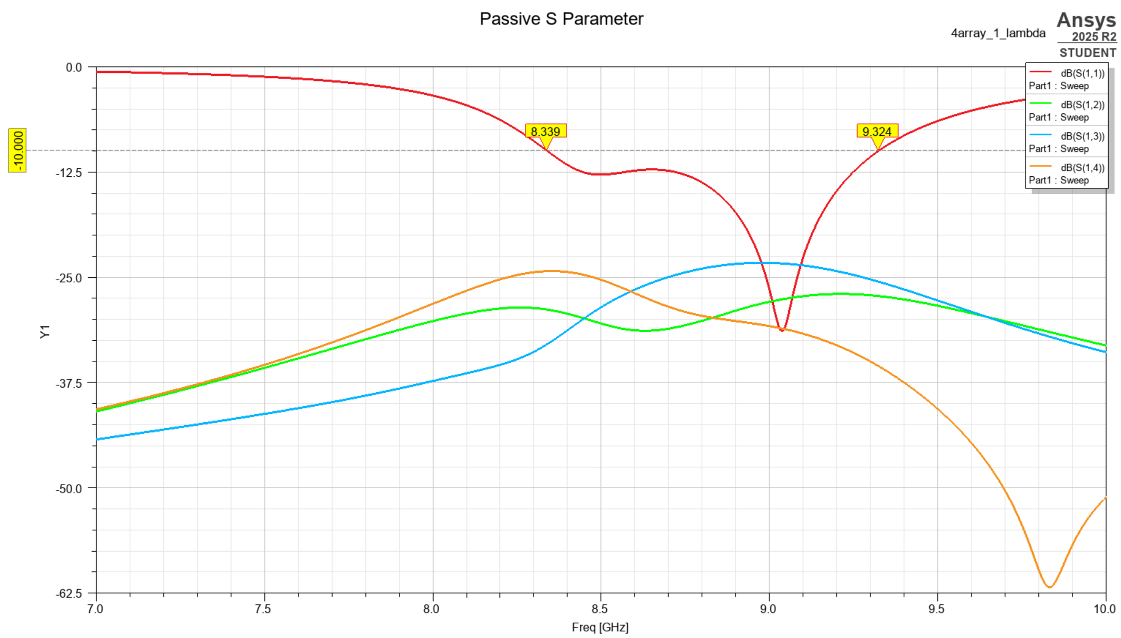

Figure 11: S-Parameter Coupling for Port-1 Excitation at λ spacing

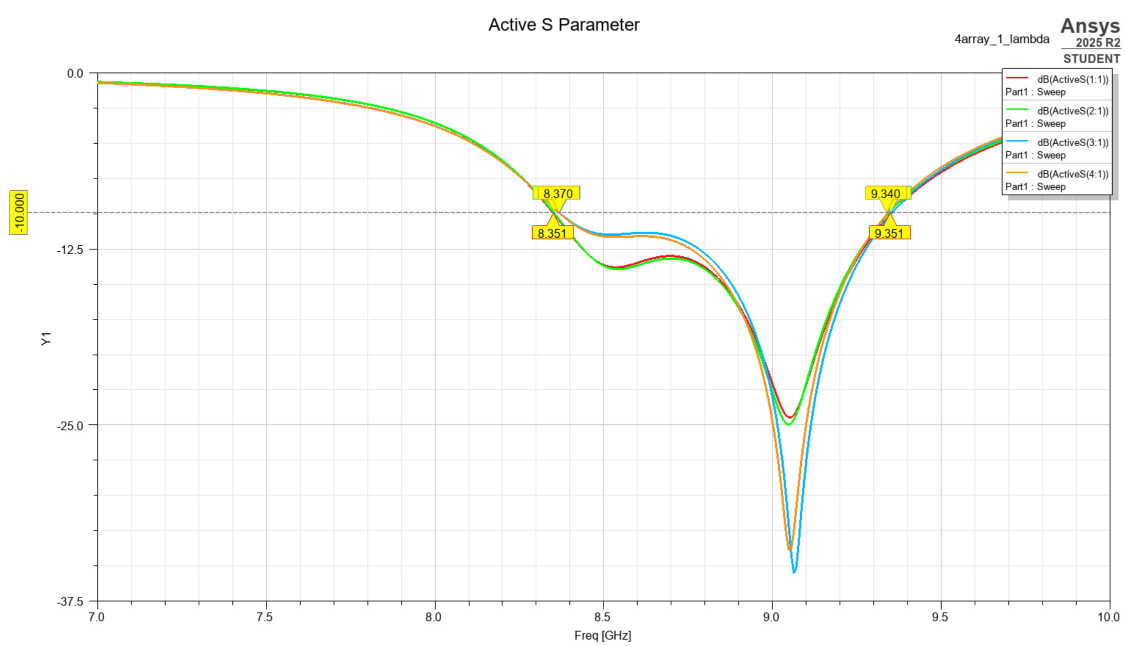

Figure 12: Active S-Parameters at λ spacing

As seen by Figure 7, Figure 9, and Figure 11, the response of the other elements due to port 1 excitation consistently remained below -20 dB, demonstrating the minimal coupling between array elements. In addition, Figure 8, Figure 10, and Figure 12 show that when all 4 elements are excited, the bandwidth for each element remains within specification.

4.3 Array Theory

The radiation patterns of the antenna array were computed using pattern multiplication, combining the single-element radiation pattern obtained from HFSS with an analytically derived array factor. The element pattern was exported from HFSS as realized gain and converted from decibel to linear power scale for use in the calculations.

For a circular array of $N = 4$ elements equally spaced on a circle of radius R, the array factor is given by:

$$AF(\theta, \phi) = \sum_{n=1}^{N} e^{jk(x_n \sin\theta \cos\phi + y_n \sin\theta \sin\phi)} \tag{13}$$

where $k = 2\pi/\lambda$ is the free-space wavenumber and (x_n, y_n) are the coordinates of the n-th element. The total realized gain of the array was then calculated using:

$$G_{\text{array}}(\theta, \phi) = G_{\text{element}}(\theta, \phi) \cdot |AF(\theta, \phi)|^2 \tag{14}$$

where G_{element} is the realized gain of the single patch antenna in linear scale. The resulting pattern was converted back to decibels for visualization.

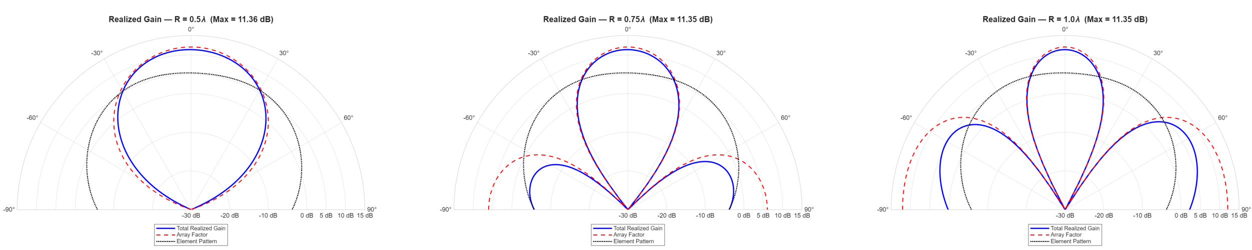

(a) 0.5λ spacing (b) 0.75λ spacing (c) λ spacing

Figure 13: Calculated total realized gain patterns in XZ Plane

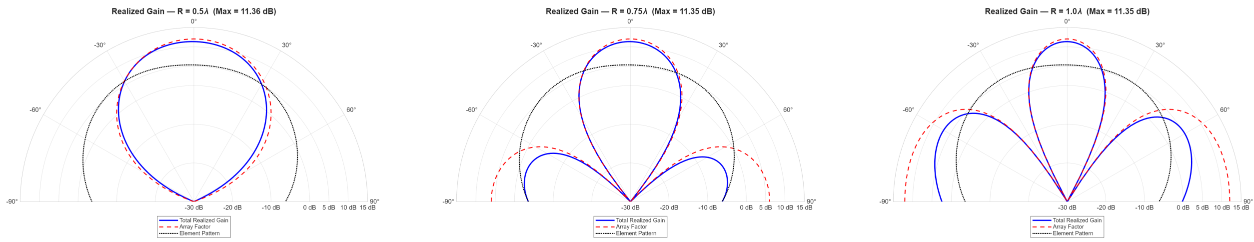

(a) 0.5λ spacing (b) 0.75λ spacing (c) λ spacing

Figure 14: Calculated total realized gain patterns in YZ Plane

4.4 Radiation Patterns

The total pattern and array factors were calculated with Matlab at 8.75 GHz for the three spacing configurations of 0.5λ, 0.75λ, and λ in both the XZ and YZ planes. These were compared with the corresponding simulated total realized gain radiation patterns.

4.4.1 0.5λ Spacing

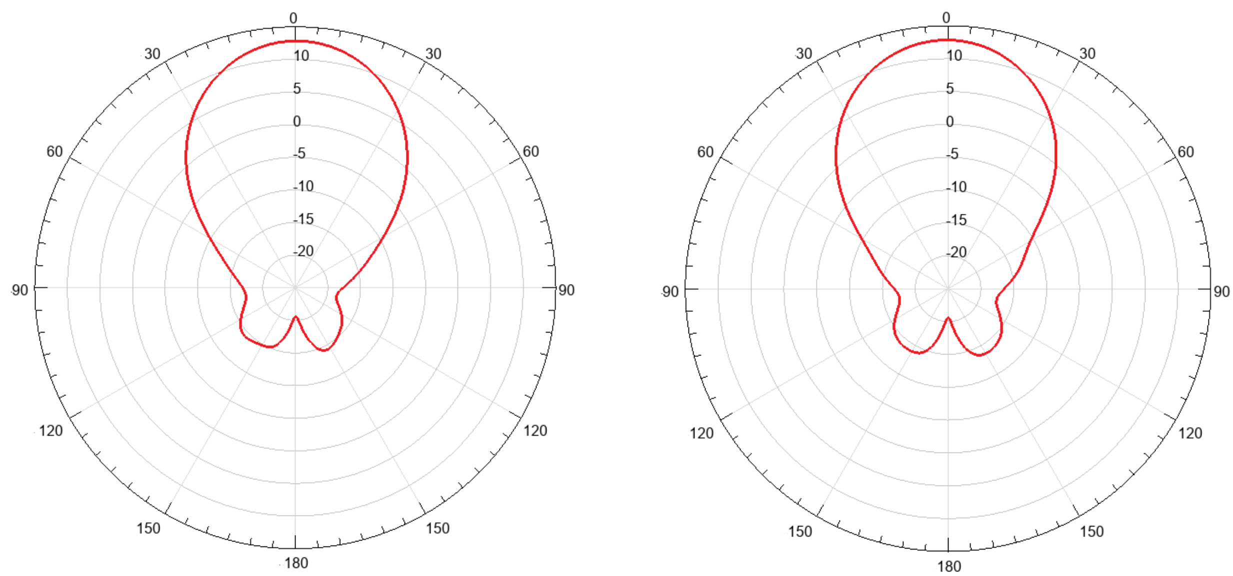

(a) XZ Plane (b) YZ Plane

Figure 15: Total realized gain pattern for 0.5λ spacing

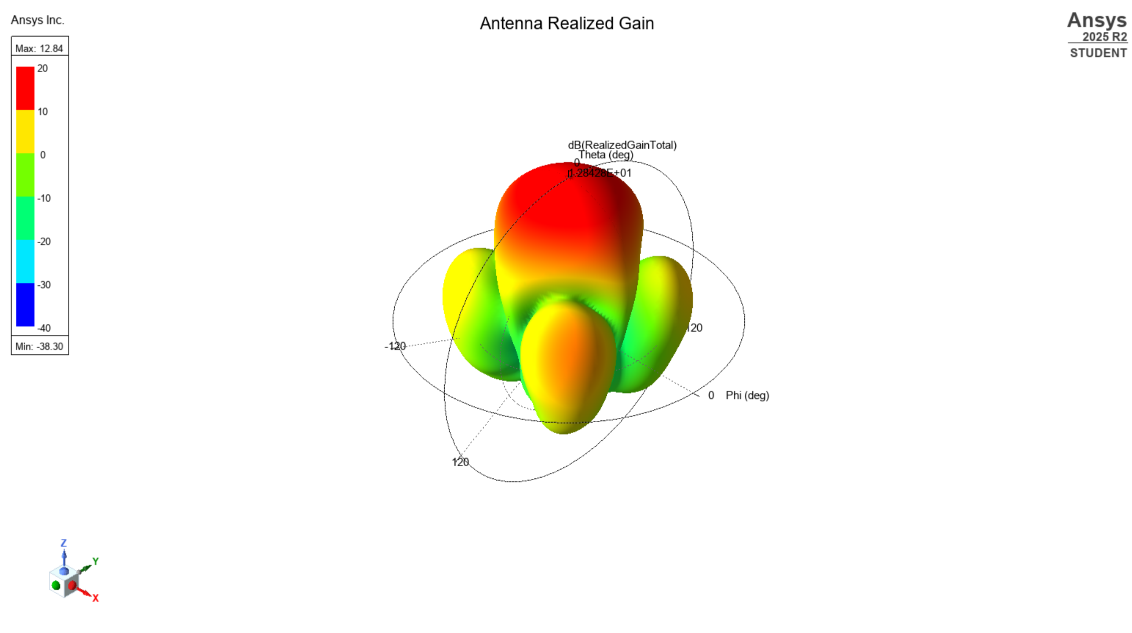

Figure 16: 3D Realized Gain Pattern for 0.5λ spacing

4.4.2 0.75λ Spacing

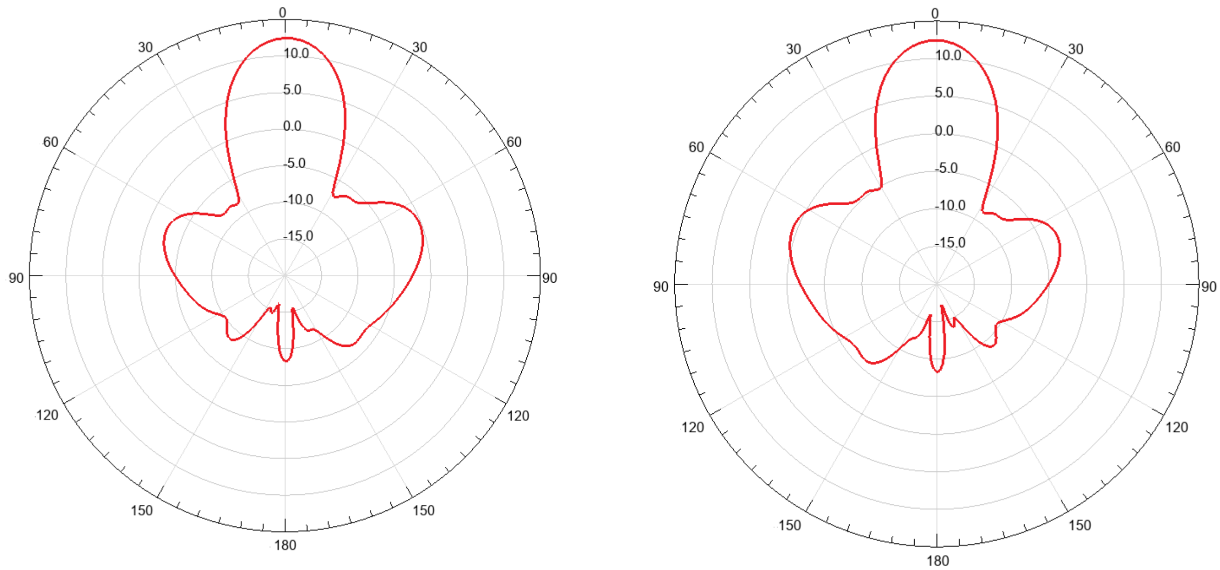

(a) XZ Plane

(b) YZ Plane

Figure 17: Total realized gain pattern for 0.75λ spacing

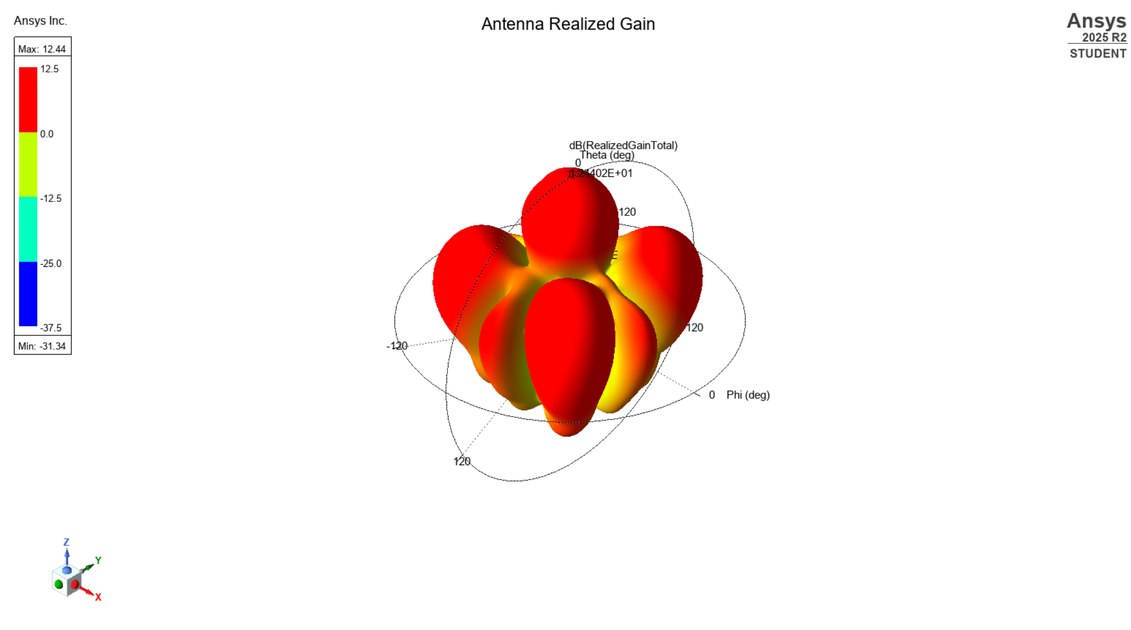

Figure 18: 3D Realized Gain Pattern for 0.75λ spacing

4.4.3 λ Spacing

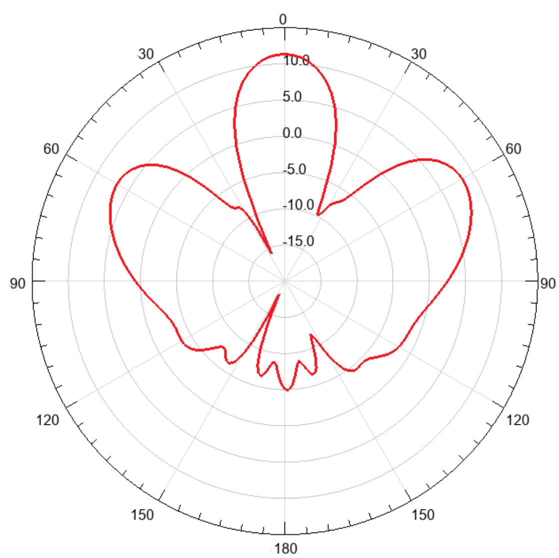

(a) XZ Plane

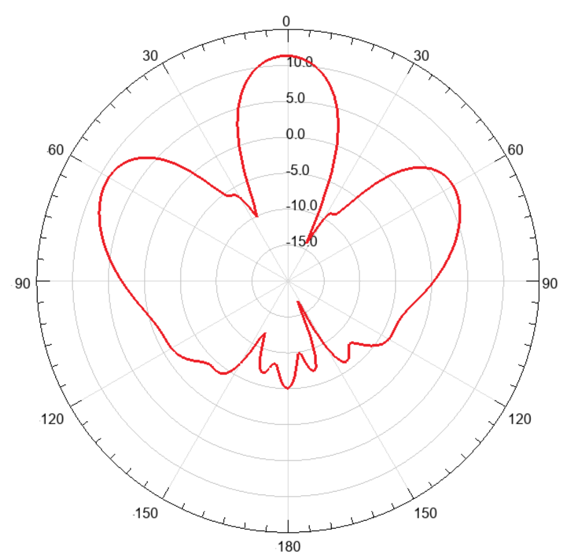

(b) YZ Plane

Figure 19: Total realized gain pattern for λ spacing

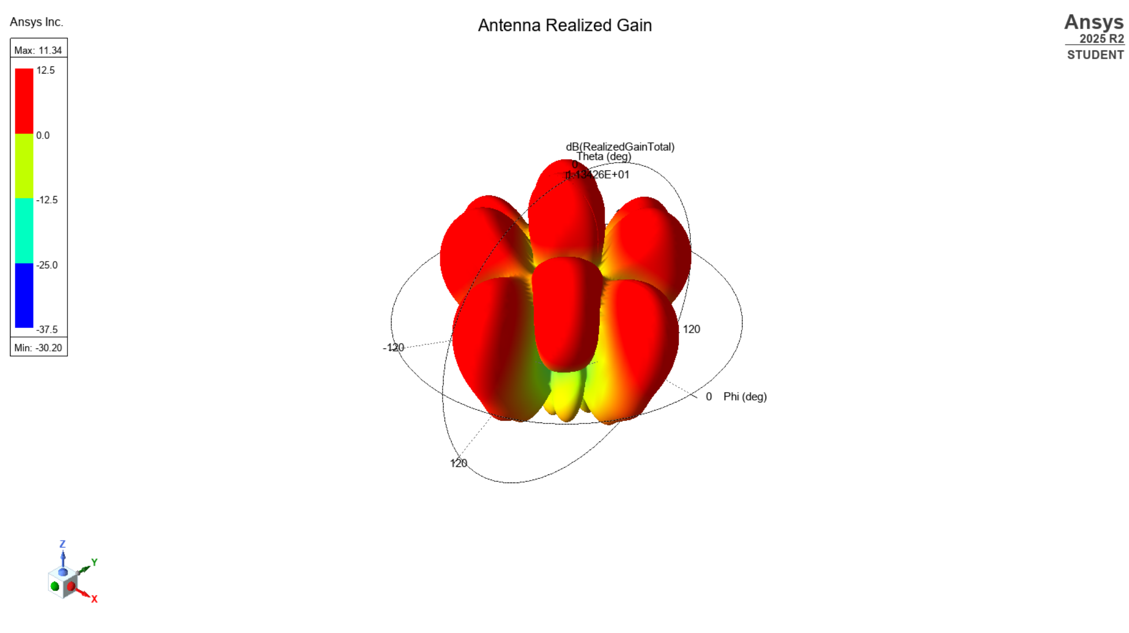

Figure 20: 3D Realized Gain Pattern for λ spacing

5 Observations and Conclusions

5.1 Single Element

The corner-chamfered patch design successfully achieved circular polarization at 8.75 GHz through perturbation of the two degenerate orthogonal modes. The non-square patch dimensions (W = 9.00 mm, L = 9.25 mm) were determined to simultaneously acheive the bandwidth and axial ratio specifications. The achieved impedance bandwidth of 8.3 – 9.3 GHz significantly exceeds the 8.5 – 9.0 GHz specification, providing comfortable fabrication margin.

The axial ratio and RHCP/LHCP isolation were found to be directly coupled through the chamfer size dL. Increasing dL improved AR at the cost of separating the two S_{11} dips and raising the mid-band peak, while decreasing dL caused the modes to merge and the axial ratio to degrade. The final chamfer of 1.8 mm was a tradeoff between CP quality and impedance bandwidth on this substrate.

5.2 4-Element Array

The HFSS simulations and theoretical Matlab calculations matched up nicely, giving similar array patterns and gains. As expected, the smaller the array radius, the higher the total realized gain. It is also important to note that the configurations of 0.75λ spacing and λ

spacing had very large sidelobes and narrow main beams compared to the 0.5λ spacing.

6 Antenna Manufacturing

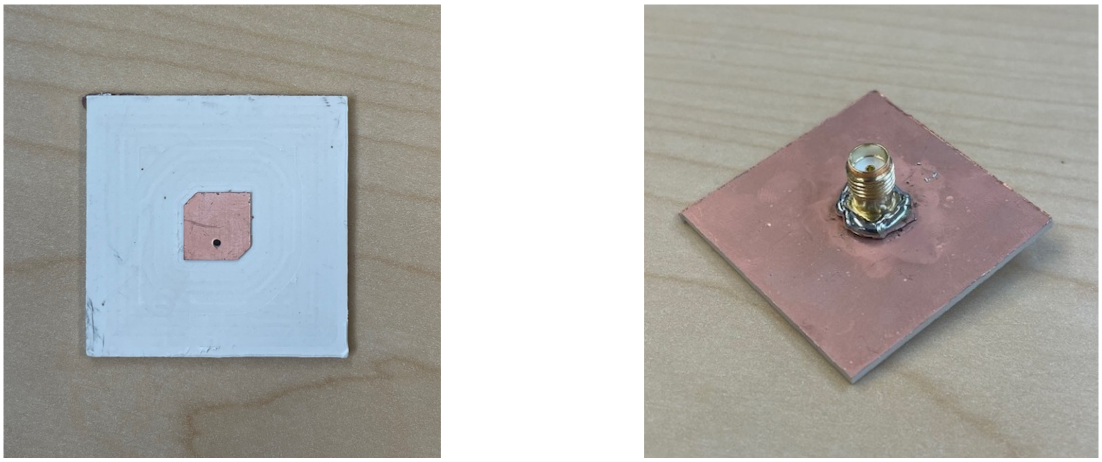

(a) Patch and Feed Hole

(b) Ground Plane and SMA Connector

Figure 21: Manufactured Single-Element Patch

The single-element patch antenna was cut out from the Rogers RO3003 substrate using a Bantam Tools Desktop CNC Milling Machine. A coaxial probe feed was implemented using an SMA connector soldered to the patch and ground plane.

6.1 Measured Results

The reflection coefficient of the fabricated antenna was measured using an R140 1-port vector network analyzer. As shown in Fig. 22, the antenna exhibits a clear resonance at approximately 9.3 GHz, which is higher than the intended design frequency of 8.75 GHz. This 9.3 GHz dip actually corresponds to the higher of the 2 resonant dips. Since the first resonant dip was shallow (around -13 dB) in simulations, it is barely noticeable in the measured response.

This frequency shift indicates that the substrate dielectric constant may have not been exactly $\varepsilon_r = 3.0$ in practice.

6.2 Parametric Study

To account for the discrepancy between simulated and measured results, a parametric study was conducted in Ansys HFSS. The goal was to identify the true dielectric constant that

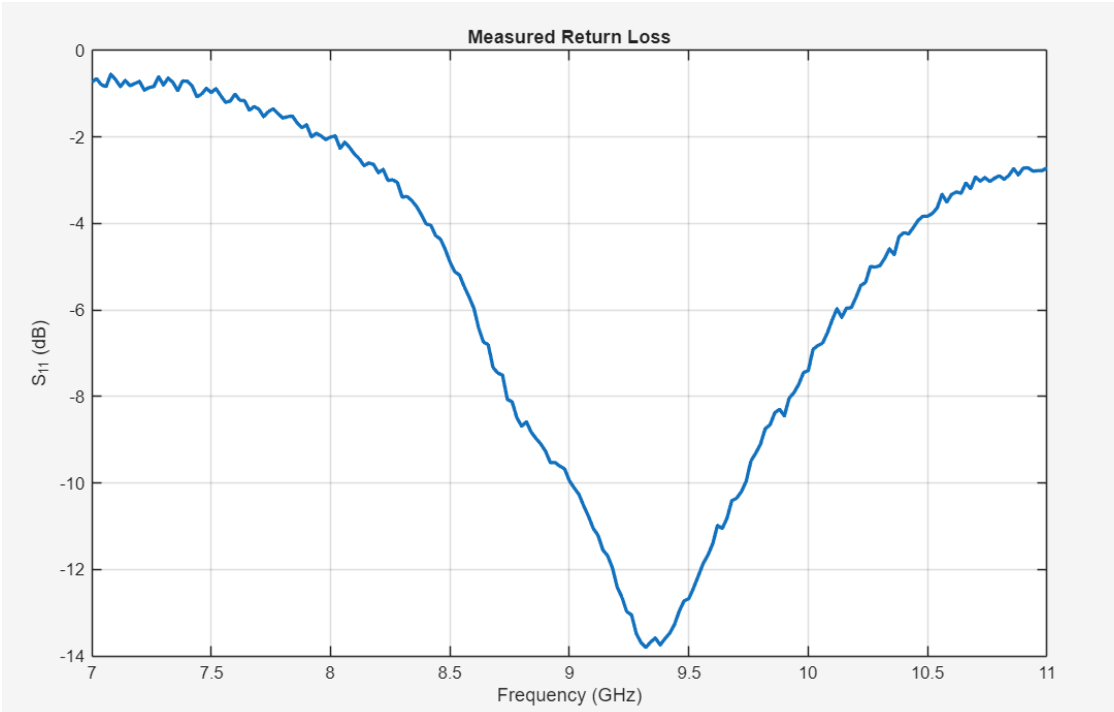

Figure 22: Measured S_{11} for the fabricated single-element patch antenna

resulted in the frequency shift in Fig. 22.

The effective dielectric constant was swept until the higher resonant dip was centered at 9.3 GHz. This was achieved with a $\varepsilon_r = 2.85$ which is a lower value than initially assumed. This corrected permittivity was then used in subsequent simulations. The new S_{11} values with the new constant can be seen in Fig. 23

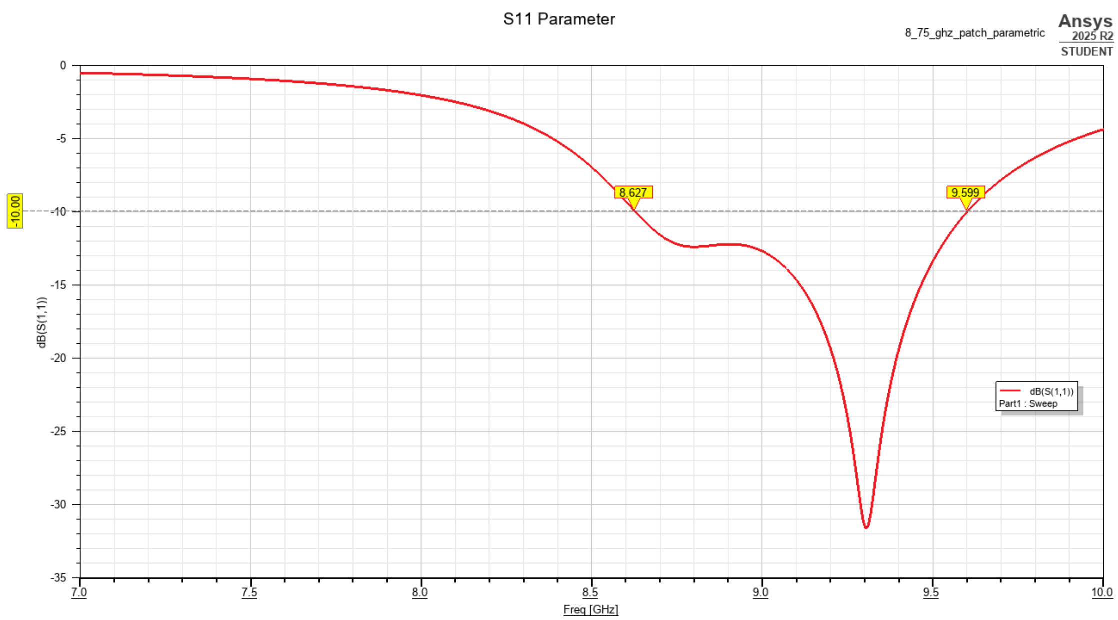

Figure 23: S_{11} values for initial patch design using $\varepsilon_r = 2.85$

7 Learning Experience

This project provided hands-on experience with antenna design, electromagnetic simulation, and electronic component manufacturing. It allowed the application of theoretical concepts to a physical engineering design.

Regarding the CAD design, the biggest insight was the physical coupling between circular polarization quality and impedance bandwidth for the patch. At first, they seemed to be independent parameters, but in simulation it became clear that both were governed by the same chamfer perturbation mechanism, making simultaneous optimization difficult to tune manually. The iterative tuning process of sweeping dL and observing the S_{11} dip splitting while also monitoring axial ratio simultaneously, gave a deeper understanding of how the two orthogonal modes interact that equations alone do not convey.

On the simulation side, the project provided practical experience with Ansys HFSS Electronics Desktop, including the setup of parametric sweeps and the use of the built-in Optimetrics framework. When the optimization wouldn't converge, it was important to understand the behavior of algorithms like gradient-based and pattern search, choose appropriate parameter starting points, and apply cost function weighting to be able to move forward.

Lastly, the physical fabrication stage also had a set of challenges. Exporting the design to Gerber files required careful attention to layer ordering and drill file formatting to ensure compatibility with the Bantam PCB mill. For testing after fabrication, the SMA connector required physical modification and the ground plane required trimming to prevent shorting between the connector body and the ground conductor. The project also provided experience with using a VNA to test the antenna and determine the measured operating frequency.

Overall, this project offered valuable experience in the full design-to-fabrication workflow for a microstrip patch antenna and array, useful in the fields of wireless communications and RF systems engineering.

A HFSS Simulation Setup Summary

Table 7: Complete Simulation Parameter Reference

Parameter	**Single Element**	**Array**
Solver	Driven Modal	Driven Modal
Center frequency	8.75 GHz	8.75 GHz
Sweep type	Discrete	Discrete
Frequency range	8.0 – 9.5 GHz	8.0 – 9.5 GHz
Frequency step	5 MHz	5 MHz
Max mesh passes	10	10
Delta S	0.02	0.02
Radiation box clearance	$\lambda/4$	$\lambda/4$
Number of ports	1	4
Far field resolution	1°	1°